IOP Publishing Physica Scripta
Phys. Scr. 95 (2020) 055811 (9pp) https://doi.org/10.1088/1402-4896/ab7aaa

Unconventional critical behavior of the magnetic refrigerant system $Er_{0.98}\square_{0.02}Co_2$ around its ferromagnetic-paramagnetic transition

R Hamdi[1,2], M Smari[2], A Bajorek[3,4], K Nouri[5], L Bessais[4], S Hayek[6], E Dhahri[2] and Y Haik[7]

[1] College of Health and Life Sciences, Hamad Bin Khalifa University, P O Box 34110, Doha, Qatar
[2] Laboratoire de Physique Appliquée, Faculté des Sciences, Université de Sfax, B P 1171, Sfax 3000, Tunisias
[3] A. Chelkowski Institute of Physics, University of Silesia, Uniwersytecka 4 St., 40-007, Katowice, Poland
[4] Silesian Center for Education and Interdisciplinary Research, University of Silesia in Katowice, 75 Pułku Piechoty 1 A, 41-500 Chorzów, Poland
[5] CMTR, ICMPE, UMR 7182 CNRS-UPEC, 2 rue Henri Dunant, F-94320 Thiais, France
[6] Department of Mechanical Engineering, University of Tabuk, Saudi Arabia
[7] College of Science and Engineering, Hamad Bin Khalifa University, P O Box 34110, Doha, Qatar

E-mail: youhaik@mail.hbku.edu.qa

Received 11 December 2019, revised 20 February 2020
Accepted for publication 27 February 2020
Published 13 March 2020

Abstract

Magnetic refrigeration is a promising energy efficient and environmentally friendly refrigeration technology. The major problem in magnetic refrigeration is to find working materials with a large magnetocaloric effect (MCE) in different temperatures regions. MCE is the reversible temperature change of a magnetic materials upon the application or removal of a magnetic field. Nanoscale magnetic materials are good candidates for magnetic refrigeration due to a presence of a large MCE in the superparamagnetic system and reduced hysteresis losses. The critical behavior of $Er_{0.98}\square_{0.02}Co_2$ intermetallic system has been investigated via isothermal magnetizations around its ferromagnetic-paramagnetic (FM-PM) transition at Curie temperature $T_C = 62$ K. This study was performed through different methods; Arrott-Noakes technique, Kouvel-Fisher analysis, and critical isotherms procedure. All these models could not explain the behavior of the studied system, which suggest that it belongs to an unconventional critical behavior. The critical exponents of the magnetization β, for the temperature dependence of the spontaneous magnetization below Curie Temperature (T_C), and γ for the magnetic susceptibility, and δ for the magnetic isotherm at T_C were calculated. Based on Modified Arrott plots; $Er_{0.98}\square_{0.02}Co_2$ gives $T_C = 62.57$ K $\pm$ 0.01 K with $\beta = 0.68 \pm 0.005$ and $T_C = 62.59$ K $\pm$ 0.01 K with $\gamma = 0.88 \pm 0.008$. Using Kouvel-Fisher technique, we get $T_C = 62.66$ K $\pm$ 0.06 K with $\beta = 0.71 \pm 0.01$ and $T_C = 62.54$ K $\pm$ 0.02 K with $\gamma = 0.90 \pm 0.06$. The extracted value of δ from the critical isotherms and the Widom scaling relation are so close confirming that the obtained critical exponents are suitable and accurate within experimental error values. With 536.45 J kg^{-1} at 5 T of relative cooling power, $Er_{0.98}\square_{0.02}Co_2$ is very promising as magnetic refrigerant.

Keywords: $ErCo_2$, critical behavior, phase transition, critical exponents, relative cooling power

(Some figures may appear in colour only in the online journal)

1. Introduction

Systems with R_MT structure (R is a Lanthanide series element of the Periodic table, e.g.: La, Pr, Nd, Pm, Sm, Lu, Y and MT is either Co or Fe) [1], present different challenging physical phenomena. The RCo_2 systems can be considered as the best model for testing and developing the theoretical notions for describing the characteristics of R_MT systems as announced by Kozlenko *et al* [1]. The RCo_2 intermetallics are very sensitive to the action of magnetic fields. Once R site contains non-magnetic element, which is generally paramagnet (PM) in nature, the induction of Co magnetization can only be achieved through applying a strong external magnetic field varying from 70 to 75 T [2]. Whilst, in case that R represents a magnetic chemical element, a ferrimagnetic (FI) state will occur between R and Co sublattices and the Co magnetic moment gets around 1 μ_B/atom at the low temperature of transition which is around 4.2 K [3, 4].

The universality class, based on the dimension of the lattice and the order of the parameter, is one of the fundamental questions related to the ferromagnetic- paramagnetic transition (FM-PM) [5, 6]. This universality class depends on the values of the critical exponents characterizing the phase transition. To understand the nature of this transition, we have discussed the critical behavior, predicting the existence of a universality class of the prepared system [7–9]. Scaling curves extracted from the isotherms of magnetizations around the critical temperature of transition have been investigated to derive the critical exponents of the magnetization β, for the temperature dependence of the spontaneous magnetization below Curie Temperature (T_C), and γ for the magnetic susceptibility, and δ for the magnetic isotherm at T_C. These critical exponents fulfill the Widom scaling law, $\delta = 1 + \gamma/\beta$.

Many studies of the critical behavior of different materials yield various values of β varying from 0.3 to 0.5. When $\beta = 0.5$, the model describes mean-field behavior; for $\beta = 0.365$, the material belongs to 3D-Heisenberg model; and finally, tricritical mean field model is described by $\beta = 0.25$. However, the 3D-Ising model is distinguished with $\beta = 0.325$ and the 3D-XY model with $\beta = 0.345$. The values of γ and δ for the initial magnetic susceptibility and the critical isotherms, respectively, can be extracted.

The RCo_2-type intermetallic compounds provide the occasion to investigate the complex magnetic interactions of the itinerant d-electron subsystem as a function of applied magnetic field [10]. Intermetallics have attracted many researchers over decades due to their exciting physical properties of different potential applications in data storage and magnetic refrigeration, etc [11]. We choosed the $Er_{0.98}\square_{0.02}Co_2$ system to be investigated in both experimental and theoretical ways because of the presence of two interacting magnetic subsystems; the localized magnetic moments of Er element and the itinerant 3d-electrons of Cobalt [3]. Likewise, Er exhibits a high magnetic moment around 9.60 μ_B, can provide very important magnetic refrigeration. Thus, it is predicted to be used as suitable magnetic refrigerant.

The main objective of this work is to investigate the critical behavior of the $Er_{0.98}\square_{0.02}Co_2$ intermetallic system near the ferro-paramagnetic transition to determine the spontaneous magnetization exponent β, the isothermal magnetic susceptibility exponent γ and the critical isotherm exponent δ via three different ways, namely: the modified Arrott plots [12], the Kouvel–Fisher method [13, 14], and the critical isotherm analysis.

2. Experimental setup

The alloy $Er_{0.98}\square_{0.02}Co_2$ (where $\square$ is an Er deficiency) was synthetized by using pure elements (99.9 wt%) Er and Co. It was melted under a high purity argon atmosphere, to prevent oxidation, by using an electric arc furnace with a non-consumable tungsten electrode. To ensure a good homogeneity, the ingot was turned over and remelted several times, then milled in steel vials hermetically sealed under an inert gas atmosphere (Ar) filled glove box with O_2 and H_2O rate of 1 ppm. For high energy ball milling process, a Fritsch planetary ball mill (Pulverisette P7) with five steel balls of 15 mm was used for 5 hours (University Paris-EST (ICMPE) CNRS Thiais-France). Consequently, powder was annealed at two different temperatures, i.e. 700 °C and 1190 °C, for 30 min The crystal structure was determined using a Bruker D8 diffractometer, at room temperature, with automatic divergence slit (Cu-Kα radiation; $\lambda = 1.54178$ Å). Magnetic measurements were carried out using a Superconducting Quantum Interference Device (SQUID) magnetometer (MPMS XL7 Quantum Design; University of Silesia-Poland).

It's worth to mention that the effective internal magnetic field H_{int}, which was utilized to determine different critical exponents, was corrected by a demagnetization factor (D) where; $H_{int} = H_{app}$-DM; D notes the demagnetization factor extracted from magnetizations versus magnetic fields measurements at the low field linear response regime at very low temperature.

3. Results and discussions

We characterized the second-order phase transition around Curie temperature T_C which will be described by three critical exponents β, γ, and δ; the spontaneous magnetization exponent β, the isothermal magnetic susceptibility exponent γ and the critical isotherm exponent δ. These parameters are expressed via the mathematical equations as following [15–21]:

$$M_S(T) = M_0(-\varepsilon)^{\beta};\ \varepsilon < 0 \tag{1}$$

$$\chi_0^{-1}(T) = \left(\frac{h_0}{M_0}\right)\varepsilon^{\gamma};\ \varepsilon > 0 \tag{2}$$

$$M = DH^{\frac{1}{\delta}};\ \varepsilon = 0 \tag{3}$$

Where M_S is the spontaneous magnetization, M_0, h_0 and D represent critical amplitudes and ε defines the reduced

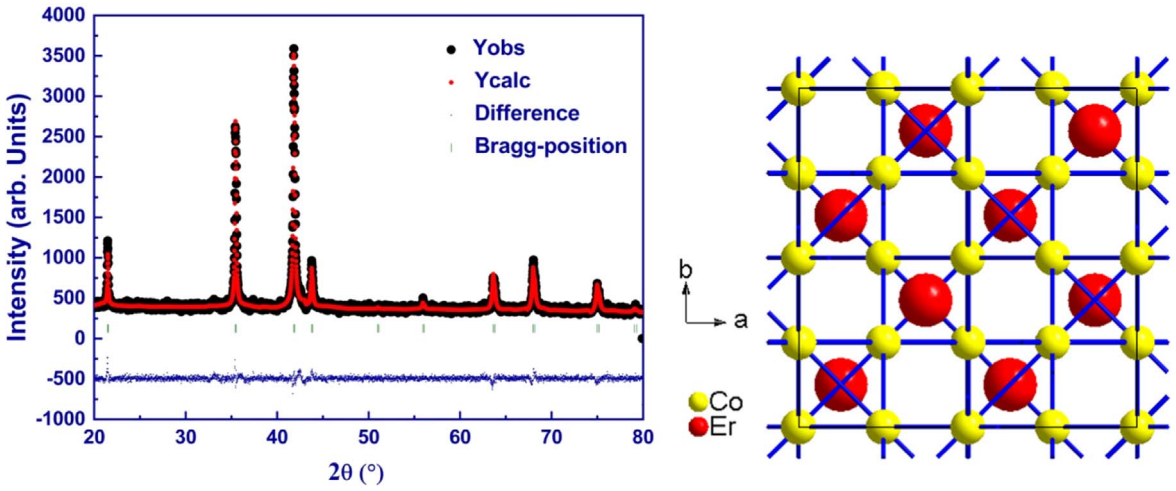

Figure 1. Rietveld refinement of the room temperature x-ray diffraction patterns (XRD) and the crystal structure of the of $Er_{0.98}\square_{0.02}Co_2$ system using Diamond - Crystal and Molecular Structure Visualization software.

temperature with $\varepsilon = (T\text{-}T_C)/T_C$. M_S was obtained through the intersection of the fitted linear isothermal magnetization curve with the $M^{1/\beta}$ axis. The same procedure was performed for $1/\chi_0$, but the intersection was with the $(H/M)^{1/\gamma}$ axis, instead. Both results were plotted as a function of temperature; M_S (T) and $1/\chi_0$(T).

Figure 1 presents the x-ray diffraction patterns (XRD) of $Er_{0.98}\square_{0.02}Co_2$ sample at room temperature in the 2θ range of 20°–80°. It illustrates a good crystallization presented by the fine line with a single-phase structure. Based on Rietveld refinement and FULLPROF software, the observed X-ray intensity with the theoretical fit and the Bragg positions are illustrated in the same figure. This refinement confirms that $Er_{0.98}\square_{0.02}Co_2$ presents a single phase, and it is indexed to the cubic structure (Fd-3m space group). After that, Diamond-Crystal and Molecular Structure Visualization software were investigated to present the crystal structure of this system, on the right-side.

Figure 2 depicts the Zero-Field-Cooling (ZFC) and Field-Cooling (FC) magnetization measurement of $Er_{0.98}\square_{0.02}Co_2$ system in temperature range span of 2–100 K at 500 Oe.

At low temperatures, the thermal evolution of ZFC/FC measurements presents an irreversible behavior that was usually considered to be as sign of the presence of spin-glass systems [22]. It is detected in many other systems, as found by Kowalczyk *et al* [22]. Still at low temperatures, the thermal magnetization M_{FC} (T) shows saturation, indicating dominance of FM behavior. The diminution in the M_{ZFC} (T) values can be attributed to the competition between magnetic domains, as found in $LuFe_{10}Mo_2$ [23].

These values of magnetization (in both ZFC and FC) begin to go lower while increasing the temperature to achieve PM state at high temperatures. Based on the first derivative of magnetization dM_{FC}/dT presenting negative values ($dM_{FC}/dT < 0$), we confirm that the sample undergoes an abrupt transition from FM state to PM order at Curie temperature $T_C = 62$ K. The T_C is also presented by the intersection point between ZFC and FC curves. Figure 2, also,

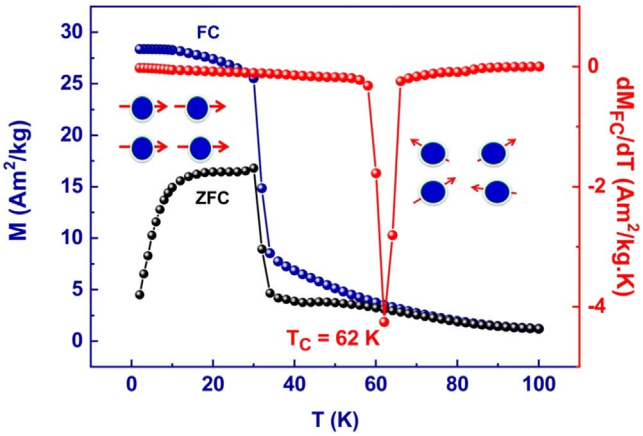

Figure 2. Thermal variation of Zero-Field-Cooling (ZFC) and Field-Cooling (FC) magnetization and its derivative dM_{FC}/dT of $Er_{0.98}\square_{0.02}Co_2$ sample at 500 Oe presenting the Curie temperature $T_C = 62$ K.

shows an approximate drawing of the spins' disposition in both cases, FM and PM states.

The hysteresis magnetizations presented in figure 3(a) show that, $Er_{0.98}\square_{0.02}Co_2$ compound presents a saturated magnetization at 5 and 10 K, confirming existence of FM order at low temperatures. Upon augmenting the temperature, the PM state is presented and illustrated by the linear variation of the magnetization versus magnetic field M versus H at 100 K. Table 1 presents the values of the coercive field (H_c), the saturation magnetization (M_{sat}) and the remanence (M_{rem}). Figure 3(b) depicts an enlarged view of M versus H to present the hysteresis.

Isothermal magnetizations of $Er_{0.98}\square_{0.02}Co_2$ system up to 7 T at the temperature range varying from 5_100 K (from 5 to 40 K by step of 5 K; from 40 K to 90 K by step of 1 K and then by step of 5 K again) are depicted in figure 4(a). At low temperature, different magnetizations are saturated exhibiting the FM behavior of this system. When the temperature increases, the isothermal variation of the magnetization tend to be linear exhibiting the PM state and confirming, thus, the

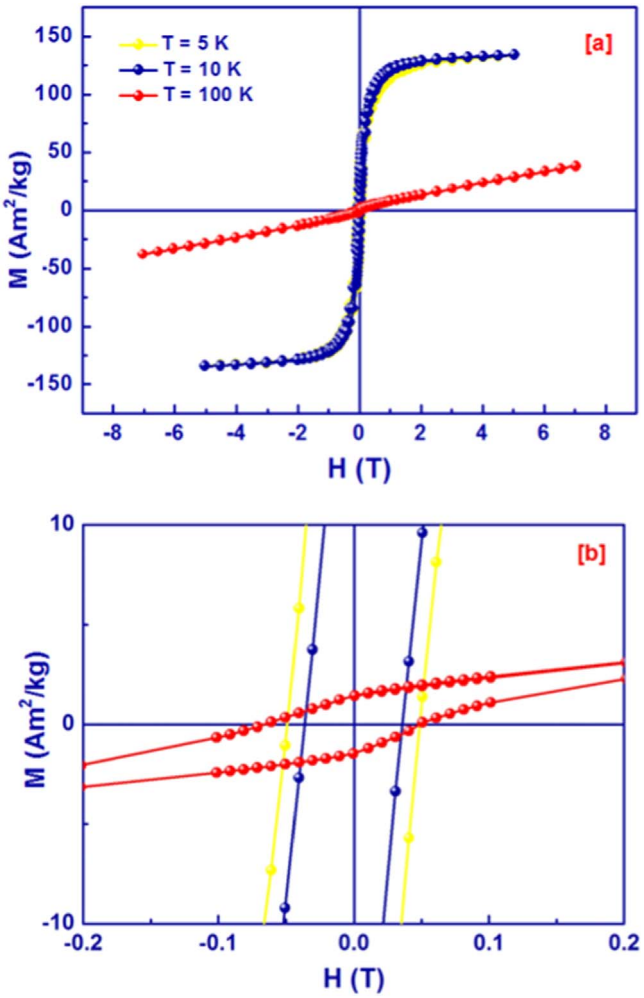

Figure 3. (a), (b): (a) Hysteresis magnetizations of $Er_{0.98}\square_{0.02}Co_2$ system versus applied magnetic field at 5, 10 and 100 K. (b) Enlarged view of M versus H.

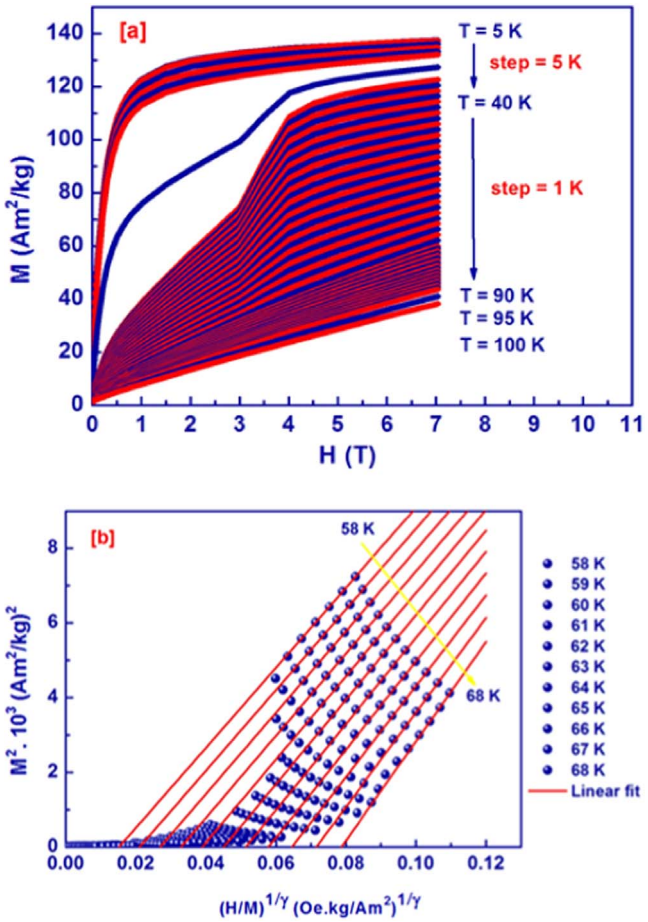

Figure 4. (a), (b): (a) Isothermal magnetization of $Er_{0.98}\square_{0.02}Co_2$ sample up to 7 T from 5 to 100 K. (b) Standard Arrott plots (M^2 versus H/M) at some temperatures around the ferro → paramagnetic transition.

Table 1. The saturation magnetization (M_{sat}), the remanence (M_{rem}) and the coercive field (H_c) of $Er_{0.98}\square_{0.02}Co_2$ system.

M_{sat} (Am^2/kg)			M_{rem} (Am^2/kg)			H_c (Oe)		
5 K	10 K	100 K	5 K	10 K	100 K	5 K	10 K	100 K
135	135	—	32	25	1.4	485	353	476

ferro-paramagnetic transition shown in figure 2. One can expect a large change in the MCE, due to the fact that magnetization changes rapidly with varying temperature, and because the MCE is temperature and magnetic field dependent. Consequently, the nature of the magnetic transition based on the criterion of Banerjee [24] was determined. The isothermal magnetizations were then converted into standard Arrott plots (M^2 versus H/M). All the curves depict positive slopes with a linear behavior at high magnetic fields presenting a second-order transition from FM-PM state (figure 4(b)).

In order to further more discuss the transition temperature of this system, we studied to which model this system belongs to and determined its critical exponents. The isothermal magnetization curves presented in figure 4(a) were used and transformed into $M^{1/\beta}$ versus $(H/M)^{1/\gamma}$ plots. This method is called Modified Arrott plots (MAP) or Arrott-Noakes plots. Figures 5(a)–(e) depicts the Arrott-Noakes plots of the prepared $Er_{0.98}\square_{0.02}Co_2$ sample. The Mean field model (Standard Arrott plots) with $\beta = 0.5$ and $\gamma = 1$ is exhibited in figure 5(a). Figure 5(b) presents 3D-Heisenberg model with $\beta = 0.365$ and $\gamma = 1.336$. Figure 5(c) shows the Tricritical mean field model with $\beta = 0.25$ and $\gamma = 1$. Figure 5(d) illustrates 3D-Ising model with $\beta = 0.325$ and $\gamma = 1.241$. 3D-XY model with $\beta = 0.345$ and $\gamma = 1.316$ is presented in figure 5(e).

All above models were unable to interpret this system due to the fact that these plots represent curved lines instead of linear ones. The unconventional critical behavior of the magnetization in the erbium compounds cannot be understood with previous theoretical interpretations of critical phenomena. Thus, this system belongs to an unconventional model with new critical exponents. We tried determining the new values of β and γ based on equations (1) and (2), which present an optimum fitting through using a self-consistent method [17, 25, 26]. Many trials were made till a convergence of these values was reached, i.e.: $\beta = 0.68$ and $\gamma = 0.88$, presented in figure 6. We concluded that, the $Er_{0.98}\square_{0.02}Co_2$

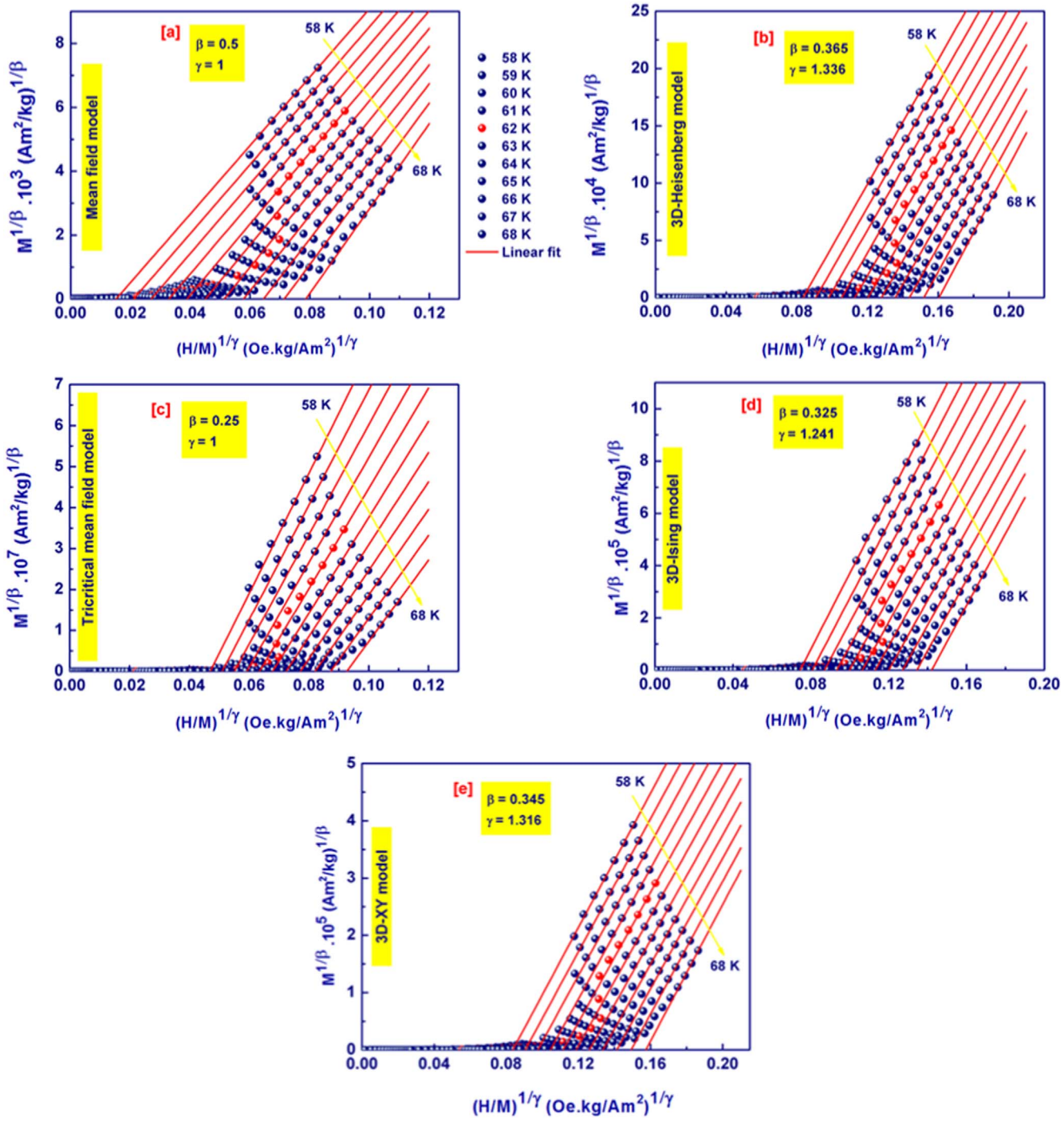

Figure 5. (a)–(e): Modified Arrott plots (MAP) of $Er_{0.98}\square_{0.02}Co_2$ sample. (a) Mean field model (Standard Arrott plots) with $\beta = 0.5$ and $\gamma = 1$. (b) 3D-Heisenberg model with $\beta = 0.365$ and $\gamma = 1.336$. (c) Tricritical mean field model with $\beta = 0.25$ and $\gamma = 1$. (d) 3D-Ising model with $\beta = 0.325$ and $\gamma = 1.241$. (e) 3D-XY model with $\beta = 0.345$ and $\gamma = 1.316$.

sample belongs to the new unconventional model. Triki *et al* [26] showed that the ferromagnet $La_{0.4}Ca_{0.6}MnO_{2.8}\square_{0.2}$ oxide belongs also to an unconventional model with $\beta = 0.79$ and $\gamma = 0.71$. Same results were found by Assoudi *et al* [17] for the $La_{0.5}Ca_{0.4}Ag_{0.1}MnO_3$ manganite. Li *et al* [27] found that the intermetallic sample DyFeAl belongs to an unconventional model also, with $\beta = 0.48$ and $\gamma = 1.33$.

After the values of β and γ were obtained, we plotted the thermal variation of the spontaneous magnetization M_S (T) and the inverse of the initial susceptibility $1/\chi_0$(T) of $Er_{0.98}\square_{0.02}Co_2$ sample, depicted in figure 7. The fitting of both curves using both equations, (1) and (2), revealed that $T_C = 62.57\,K \pm 0.01\,K$ with $\beta = 0.68 \pm 0.005$ and $T_C = 62.59\,K \pm 0.01\,K$ with $\gamma = 0.88 \pm 0.008$, respectively. This confirmed that, the transition temperature is, approximately, 62 K as determined from the FC measurements (figure 2).

To fulfil the values of T_C, β and γ via Kouvel-Fisher method, we analyzed both the thermal variation of the

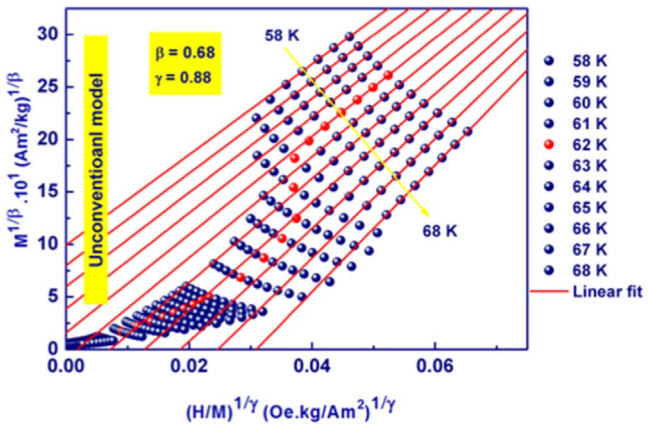

Figure 6. Unconventional model of $Er_{0.98}\square_{0.02}Co_2$ sample with $\beta = 0.68$ and $\gamma = 0.88$.

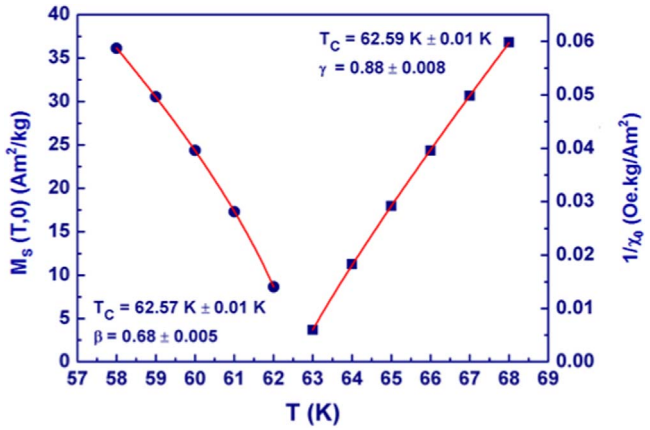

Figure 7. The spontaneous magnetization M_S (closed circles_left side) and the inverse of the initial susceptibility $1/\chi_0$ (closed squares_right side) of $Er_{0.98}\square_{0.02}Co_2$ sample with $\beta = 0.68$ and $\gamma = 0.88$. Red lines are the fits via equations (1) and (2).

spontaneous magnetization M_S (T) and the inverse of the initial susceptibility $1/\chi_0$(T) using the following expressions [13, 14]:

$$\frac{M_S(T)}{dM_S(T)/dT} = \frac{T - T_C}{\beta} \tag{4}$$

$$\frac{\chi_0^{-1}(T)}{d\chi_0^{-1}(T)/dT} = \frac{T - T_C}{\gamma} \tag{5}$$

Figure 8 depicts the thermal variation of both $M_S/(dM_S/dT)$ and $(1/\chi_0)/(d(1/\chi_0)/dT)$ via Kouvel-Fisher technique. Both plots show a linear behavior with $1/\beta$ and $1/\gamma$ as slopes. Fitting using equations (4) and (5) leads to $T_C = 62.66\,K \pm 0.06\,K$ with $\beta = 0.71 \pm 0.01$ and $T_C = 62.54\,K \pm 0.02\,K$ with $\gamma = 0.90 \pm 0.06$, respectively. These new results are so close to that extracted from Arrott-Noakes technique.

Based on equation (3), the critical isotherm exponent δ can be extracted as presented in figure 9 showing the variation of magnetization versus applied magnetic field for $T_C = 62\,K$

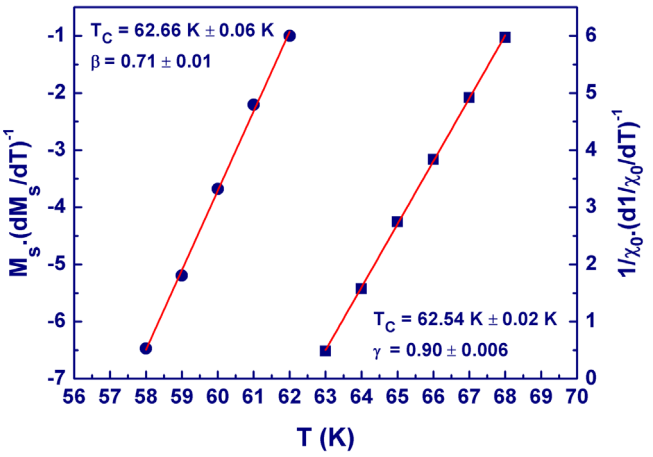

Figure 8. Kouvel-Fisher plots for $M_S/(dM_S/dT)$ (closed circles_left side) and for $(1/\chi_0)/(d(1/\chi_0)/dT)$ -(closed squares_right side) of $Er_{0.98}\square_{0.02}Co_2$ sample with $\beta = 0.71$ and $\gamma = 0.90$. Red lines are the fits via equations (4) and (5).

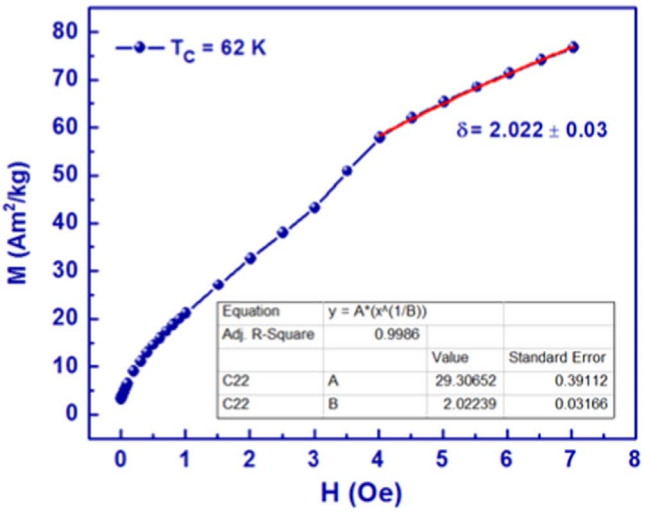

Figure 9. Magnetization versus magnetic field (M versus H) plot at $T_C = 62\,K$ of $Er_{0.98}\square_{0.02}Co_2$ sample with the fit following equation (3) giving $\delta = 2.022 \pm 0.03$.

yield in, $\delta = 2.022 \pm 0.03$. δ value was also, determined using Widom scaling relation [28]:

$$\delta = 1 + \frac{\gamma}{\beta} \tag{6}$$

Based on the values of β and γ determined through Arrott-Noakes and Kouvel-Fisher procedures presented in figures 7 and 8, equation (6) yields $\delta = 2.29$ and 2.26, respectively. Thus, the three δ values, obtained from the critical isotherms and the Widom scaling relation are so close to each other, proving that the obtained critical exponents are suitable and accurate within the accepted experimental errors. Accordingly, the critical exponents β, γ and δ and the value of T_C for this system are self-consistent and precious. Table 2 summarizes the critical exponents values through Arrott-Noakes plot, Kouvel–Fisher procedure and the critical isotherms of the $Er_{0.98}\square_{0.02}Co_2$ system.

Table 2. Critical exponents via Arrott-Noakes plots, Kouvel–Fisher procedure and critical isotherms of $Er_{0.98}\square_{0.02}Co_2$ system.

Arrott-Noakes procedure			Kouvel-Fisher technique			Critical isotherms
β	γ	δ	β	γ	δ	δ
0.68 ± 0.005 with $T_C = 62.57\,K \pm 0.01\,K$	0.88 ± 0.008 with $T_C = 62.59\,K \pm 0.01\,K$	2.29 using Widom scaling	0.71 ± 0.01 with $T_C = 62.66\,K \pm 0.06\,K$	0.90 ± 0.06 with $T_C = 62.54\,K \pm 0.02$	2.26 using Widom scaling	2.022 ± 0.03

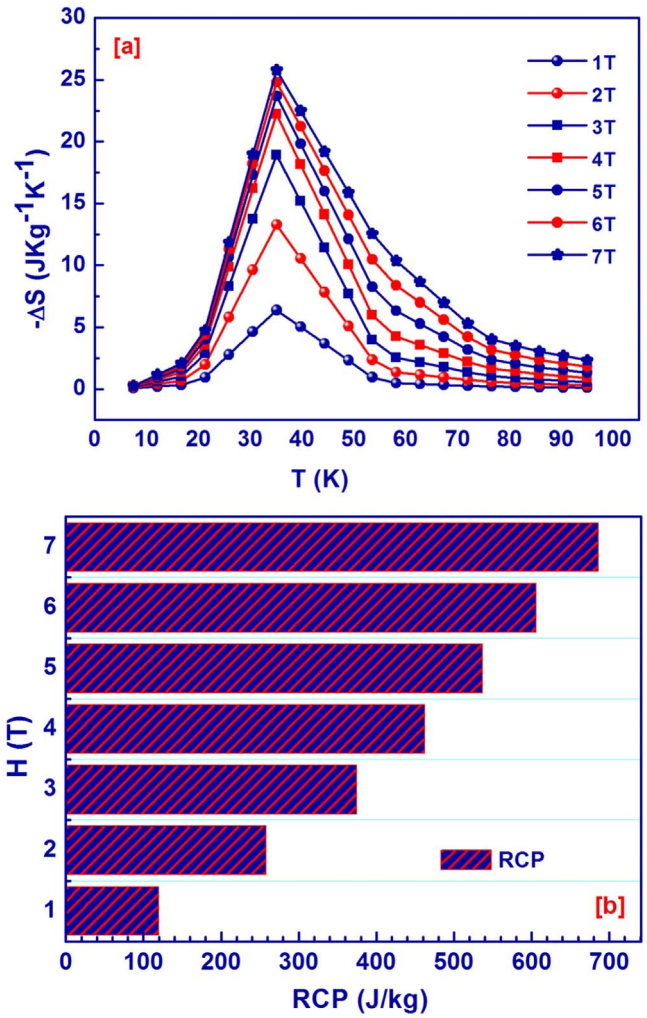

Figure 10. (a), (b): (a) Isomagnetic entropy change –ΔS from 1 to 7 T and (b) the RCP of $Er_{0.98}\square_{0.02}Co_2$ system.

After extracting the critical exponents and showing that the studied system presents an unconventional critical behavior around its FM_PM transition temperature T_C, we shall now investigate its magnetocaloric properties according to the thermodynamic Maxwell relation [29, 30]:

$$\Delta S(T, \Delta H) = \mu_0 \int_0^H \left(\frac{\partial M(T, H)}{\partial T}\right)_H dH \qquad (7)$$

Where S is the magnetic entropy of the system, H is the magnetic field, M the magnetization, T is the temperature and μ_0 represents the magnetic permeability.

Based on the isothermal magnetizations, we determined the thermal variation of the magnetic entropy change –ΔS of $Er_{0.98}\square_{0.02}Co_2$ via Maxwell's relation (7) as posted in figure 10(a). Increasing the applied magnetic field from 1 up to 7 T, a considerable MCE was detected in this system. The maximum of –ΔS increases considerably from about 6.3 J kg^{-1} K^{-1} to around 25.91 J kg^{-1} K^{-1} at 1 and 7 T, respectively.

To determine the amount of heat transfer between hot and cold reservoirs, we introduce the most valuable parameter to evaluate the capacity of the material to be as magnetic refrigerant; the relative cooling power (RCP), expressed as follows [31, 32]:

$$RCP = -\Delta S.\delta T_{FWHM} \qquad (8)$$

With $-\Delta S_{max}$ represents the maximum value of –ΔS and δT_{FWHM} is the full width at half maximum.

The RCP presents 119.83 J/k g, 536 .45 J kg^{-1}, 605.61 J kg^{-1}, and 685.83 J/kg for 1, 5, 6 and 7 T, respectively (figure 10(b)). All these results are comparable with or even higher than the best-known magnetic refrigerants; e.g.: Gd with 556 J kg^{-1} [33] and $Gd_5Si_2Ge_2$ with 305 J kg^{-1} [34]. Based on above results, $Er_{0.98}\square_{0.02}Co_2$ could be a very promising candidate for magnetic cooling technique to be used as magnetic refrigerant.

4. Conclusion

$Er_{0.98}\square_{0.02}Co_2$ system exhibits a ferromagnetic-paramagnetic (FM-PM) transition at around 62 K. It undergoes rather a second order transition. The modified Arrott plots, Kouvel-Fisher and the isotherms analysis could not explain its behavior; it may belong to an unconventional critical behavior. The unconventional critical behavior of the magnetization in the erbium compounds could not be explained with previous theoretical interpretations of critical phenomena. The analysis of the magnetic entropy change led to the conclusion that $Er_{0.98}\square_{0.02}Co_2$ system could be used as a promising magnetic refrigerant candidate in the magnetic cooling technique.

ORCID iDs

L Bessais https://orcid.org/0000-0001-7236-1604
E Dhahri https://orcid.org/0000-0002-6919-8778
Y Haik https://orcid.org/0000-0002-3665-7456

References

[1] Kozlenko D P, Burzo E, Vlaic P, Kichanov S E, Rutkauskas A V and Savenko B N 2015 *Sci. Rep.* **5** 8620
[2] Goto T, Sakakibara T, Murata K, Komatsu H and Fukamichi R 1990 *J. Magn. Magn. Mater.* **90–91** 700–2
[3] Baranov N V and Pirogov A N 1995 *J. Alloys Compd.* **217** 31–7
[4] Bloch D, Edwards D M, Shimizu M and Voiron J 1975 *J. Phys. F: Met. Phys.* 5–1217
[5] Khlifi M, Tozri A, Bejar M, Dhahri E and Hlil E K 2012 *J. Magn. Magn. Mater.* **324** 2142–6
[6] Smari M, Walha I, Omri A, Rousseau J J, Dhahri E and Hlil E K 2014 *Ceram. Int.* **40** 8945–51
[7] Rachid F Z, Omari L H, Yamkane Z, Lassri H, Derkaoui S, Nouri K, Bouzidi W and Bessais L 2019 *Mater. Chem. Phys.* **228** 60–5
[8] Madhumita Halder S M, Yusuf and Mukadam M D 2010 *Phys. Rev. B* **81** 174402
[9] Liu B, Zou Y, Zhang L, Zhou S, Wang Z, Wang W, Qu Z and Zhang Y 2016 *Sci. Rep.* **6** 33873

[10] Cuong T D, Havela L, Sechovsky V, Andreev A V, Arnold Z, Kamarad J and Duc N H 1997 *J. Appl. Phys.* **81** 4221
[11] Nouri K, Jemmali M, Walha S, Zehani K, Bessais L and Salah A B 2016 *J. Alloys Compd.* **661** 508–15
[12] Arrott A and Noakes J E 1967 *Phys. Rev. Lett.* **19** 786–9
[13] Kouvel J S and Fisher M E 1964 *Phys. Rev. A* **136** 1626–32
[14] Fisher M E, Ma S K and Nickel B G 1972 *Phys. Rev. Lett.* **29** 917
[15] Phan T L, Thanh P Q, Sinh N H, Lee K W and Yu S C 2011 *Curr. Appl Phys.* **11** 830
[16] Kim D, Revaz B, Zink B L, Hellman F, Rhyne J J and Mitchell J F 2002 *Phys. Rev. Lett.* **89** 227202
[17] Assoudi N, Smari M, Walha I, Dhahri E, Shevyrtalov S, Dikaya O and Rodionova V 2018 *Chem. Phys. Lett.* **706** 182–8
[18] Kowalczyk A, Baszyfiski J, Kovac J and Szlaferek A 1997 *J. Magn. Magn. Mater.* **176** 241–7
[19] Christides C, Kostikas A, Zouganelis G, Psyharis V, Kou X C and Grossinger R 1993 *Phys. Rev. B* **47** 11220
[20] Banerjee B K 1964 *Phys. Lett.* 12–6
[21] Padmanabhan B, Bhat H L, Elizabeth S, Rößler S, Rößler U K, Dörr K and Müller K H 2007 *Phys.Rev.B* **75** 024419
[22] Triki M, Dhahri E and Hlil E K 2013 *J. Solid State Chem.* **201** 63–7
[23] Li L, Huo D, Qian Z and Nishimura K 2014 *Intermetallics* **46** 231e235
[24] Widom B 1965 *J. Chem. Phys.* **43** 3892
[25] Hamdi R, Tozri A, Dhahri E and Bessais L 2017 *Chem. Phys. Lett.* **680** 94–100
[26] Smari M, Walha I, Dhahri E and Hlil E K 2013 *J. Alloys Compd.* **579** 564–71
[27] Smari M, Hamdi R and Dhahri E *J. Supercond. Nov. Magn.* (https://doi.org/10.1007/s10948-017-4183-5)
[28] Hamdi R, Tozri A, Smari M, Dhahri E and Bessais L 2017 *J. Magn. Magn. Mater.* **444** 270–9
[29] Gschneidner K A Jr, Pecharsky V K and Tsoko A O 2005 *Rep. Prog. Phys.* **68** 1479
[30] Pecharsky V K and Gschneidner K A Jr 1997 *Phys. Rev. Lett.* **78** 4494
[31] Moutis N, Panagiotopoulos I, Pissas M and Niarchos D 1999 *Phys. Rev. B* **59** 1130
[32] Yang J and Lee Y P 2007 *Appl.Phys.Lett.* **91** 142512
[33] Stanley H E 1971 *Introduction to Phase Transitions and Critical Phenomena* (London: Oxford University Press)
[34] Tozri A, Dhahri E and Hlil E K 2011 *Phys. Lett. A* **375** 1528–33